Environmental Science & Technology

pubs.acs.org/est

Article

Exploring Long-Term Changes in Silicon Biogeochemistry Along the River Continuum of the Rhine and Yangtze (Changjiang)

Xiaochen Liu,* Wim Joost van Hoek, Lauriane Vilmin, Arthur Beusen, José M. Mogollón, Jack J. Middelburg, and Alexander F. Bouwman

Cite This: *Environ. Sci. Technol.* 2020, 54, 11940−11950

Read Online

ACCESS | Metrics & More | Article Recommendations | Supporting Information

ABSTRACT: This paper presents the spatially explicit (0.5° spatial resolution) Dynamic InStream Chemistry (DISC)-SILICON module, which is part of the Integrated Model to Assess the Global Environment-Dynamic Global Nutrient Model global nutrient cycling framework. This new model, for the first time, enables to integrate the combined impact of long-term changes in land use, climate, and hydrology on Si sources (weathering, sewage, and soil loss) and sinks (uptake by diatoms, sedimentation, and burial) along the river continuum. Comparison of discharge and dissolved silica results with observations shows good agreement both in the Rhine and Yangtze. The simulated total Si export for the Rhine is stable during the period 1900−2000. The total Si export for the Yangtze decreased (155−51 Gmol yr^{-1}) because of damming and transformation of 40% of the natural vegetation to cropland. As a result of dam construction in the Yangtze, diatom primary production (from 24 to 48 Gmol yr^{-1}) and burial (15 to 32 Gmol yr^{-1}) increased and the DSi export decreased (139−46 Gmol yr^{-1}) from the 1950s to 1990s. The Three Gorges Reservoir has a large contribution to diatom primary production (11%) and burial (12%) in the Yangtze basin. DISC-SILICON reproduces a flooding-induced increase in Si inputs and burial and the legacy of this temporary storage in subsequent dry years.

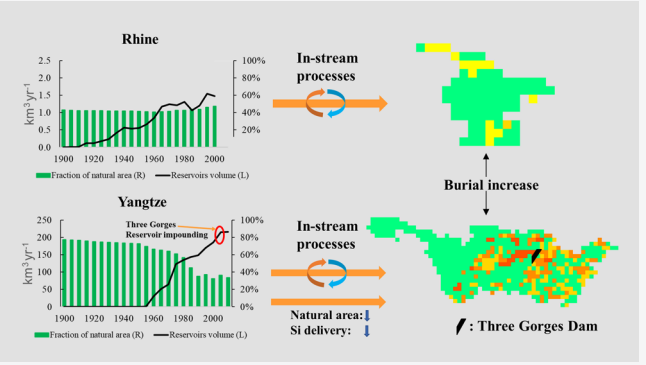

1. INTRODUCTION

Silicon (Si) occurs in the Earth's crust primarily as silicate minerals in igneous, sedimentary, and metamorphic rocks. Weathering of silicate minerals is the ultimate source of dissolved silicate (DSi) in rivers and the global ocean.[1−3] Terrestrial vegetation incorporates Si in phytoliths, forming biogenic silica (BSi). BSi stored in plants and soils can be transported to streams and rivers by surface runoff and erosion and can dissolve to form DSi.[4−6] DSi is required for the growth of siliceous algae (diatoms), an important phytoplankton group that uses Si to build their external skeleton (frustule). A change in DSi availability thus directly influences phytoplankton composition and overall primary production (PP) in both inland and coastal marine waters.[7,8]

Anthropogenic perturbations impact DSi delivery to rivers and transport through the river continuum, including land use change, dam construction, and nutrient loading to rivers. BSi and DSi are connected via precipitation, dissolution, and uptake by plants and diatoms.[9] Land use has a major impact on the mobilization of Si in river basins through its impact on all these processes.[9,10] Silicate weathering rates are higher in forests compared to cropland,[11,12] leading to high uptake rates and transformation to BSi in phytoliths (in plant biomass and via litter in soil organic matter). DSi stemming from rock weathering is thus cycled in the soil-plant system. A small part of the Si stored in soils can be lost via surface runoff and erosion and delivered to surface water.[6]

Human perturbation has major consequences for the riverine Si cycle in several ways: (i) By transforming natural vegetation to cropland or grassland, the soil-plant Si cycle is perturbed by harvesting the crop or grass biomass and thus removing BSi. Enhanced soil erosion from agricultural fields will further deplete the soil BSi pool,[9] which eventually leads to reduced Si delivery to surface water. (ii) By constructing reservoirs, the water travel time increases, which causes an increase in DSi retention because of burial of BSi in dead diatoms.[13−18] Sediments in lakes and reservoirs are thus (temporary) BSi stores which by dissolution can be a source of DSi.[19] (iii) By enhanced nutrient loading from agriculture and

Received: March 9, 2020
Revised: July 28, 2020
Accepted: August 26, 2020
Published: August 26, 2020

wastewater, which causes eutrophication. Eutrophication enhances DSi retention in reservoirs, as increasing nitrogen (N) and phosphorus (P) inputs stimulate diatom growth.[19] As a result, the molar N/Si and P/Si ratios in the water transported to the coastal ocean in dammed rivers is often higher than those in the predam situation.[20] The overall result of all these processes is an excess of N and P over the requirements of diatoms. This causes proliferation of non-diatom phytoplankton and may eventually lead to harmful algal blooms (HABs)[4,21−27] in the coastal ecosystem.

Since the first observations of DSi concentrations in rivers,[28] a series of studies focused on the global Si budget and retention in lakes and reservoirs.[29−32] There is an increasing interest in understanding the changing DSi loads of the world's rivers, lakes, and reservoirs and their relation to anthropogenic changes.[13,14,16,33−35] Future plans for the construction of a series of dams in the Yangtze river and other rivers worldwide,[36] changing climate, and continued land-use changes are a major cause of concern. Models are often used to study the impact of anthropogenic influences on riverine Si biogeochemistry. Beusen et al.[16] developed a river-basin scale multiple regression model to describe global river export of dissolved DSi. Laruelle et al.[30] and Dürr et al.[31] presented a global Si box model to estimate Si retention and export. Maavara et al.[13] developed a process-based model of Si retention in global reservoirs. All the abovementioned global approaches generate snap-shot estimates for a single year and lack long-term variation. Furthermore, these studies are based on poorly constrained hydrology and lack the spatial distributions of the controls of Si supply from weathering, the impact of land use change, the temporary storage of Si in sediment, and the in-stream biogeochemistry in streams, rivers, lakes, and reservoirs.

We therefore need a spatially explicit, process-based biogeochemistry model that can describe diatom production and DSi uptake, decay of diatoms, BSi dissolution, and Si transformations under decade-long human interferences to include the impact of large-scale accumulation or depletion of Si stores in soils of the watershed or in sediment. We developed the biogeochemistry module Dynamic InStream Chemistry (DISC)-SILICON, which is part of the Integrated Model to Assess the Global Environment (IMAGE)-Dynamic Global Nutrient Model (IMAGE-DGNM).[37] Within IMAGE-DGNM, DISC-SILICON describes the supply and processing of Si, considering long-term (20th century) changes in land use, climate, and hydrology to link Si sources (weathering, sewage, and soil erosion) and sinks (uptake by diatoms, sedimentation, and burial) for every global 0.5 by 0.5° grid cell.

We tested whether our model reproduces the observed long-term changes in the riverine Si cycle as influenced by human activities for two major rivers with contrasting geohydrological conditions, history of land use change, and dam construction, that is, the Rhine and Yangtze (Changjiang) (see Table S4, Supporting Information 4). The Yangtze River is the largest river in the Eurasian continent, with an average annual discharge of 892 $km^3\ yr^{-1}$ (1950−2000), covering an area of $1.8 \times 10^6\ km^2$ and with a length of 6400 km.[38] It hosts 35% of China's population and receives 32% of the total Chinese fertilizer inputs.[39] Expansion of agricultural land in the Yangtze basin has been dramatic during the 20th century,[40] and the construction of a series of major and minor dams has drastically changed the hydrology.[19] The most recent dam is the Three Gorges Dam that led to the formation of the Three Gorges Reservoir (TGR) in the Yangtze valley with a length of 550 km. The water level reached 175 m after filling between 2003 and 2009 and with a TGR capacity of 39 km^3, and the total reservoir capacity in the Yangtze river basin reached 142 km^3.[15] The Rhine River is the second-longest river in western and Central Europe, with an average annual discharge of 75 km^3, a length of 1350 km and, and an area coverage of 185,620 km^2.[41] The Rhine drains intensive agricultural land and strongly urbanized areas and hosts 58 million inhabitants.[42] In contrast to the Yangtze, the river Rhine has not experienced important forest clearing to expand agricultural land during the 20th century, has a series of small dams,[43] and has no major dams.[43]

2. METHODS

2.1. Model Description. *2.1.1. General Aspects.* IMAGE-DGNM[44] is a global, spatially explicit coupled nutrient cycling−hydrology model, which calculates nutrient delivery, in-stream retention, and export to the coastal ocean. This model is inspired by the Riverstrahler model[45,46] which also couples hydrology and biogeochemistry. In Riverstrahler, the inputs of all stream segments of the same Strahler order are lumped within a sub-basin. Instead, in DGNM, every grid cell has its specific environmental, hydrological, and land use conditions. In IMAGE-DGNM (Figure S1), the spiraling method for calculating in-stream retention is replaced by the process-based biogeochemical module DISC.[37] All data used in the model have a 0.5 by 0.5 spatial degree resolution. The temporal resolution is variable, selected on the basis of the process considered, and here, we use an output time step of one year.

In the framework, IMAGE-DGNM provides data to DISC on (i) spatial land cover, climate, and water use, (ii) spatial distributions of population density as a source of Si in wastewater, (iii) Si flows via soil loss to surface water, and (iv) soil types and lithology as a source of DSi weathering (Figure S1). The hydrology model PCR-GLOBWB[47,48] provides runoff, waterbody area and volume, discharge, and flow direction for the Strahler stream orders ≥6, while simulation of hydrology for the smaller stream order (<6) hydrology is parameterized following Wollheim et al.,[21] as described in detail by Beusen et al.[44] An important feature is that the history of dam construction is captured using data on the date of construction and filling, reservoir area, and depth and volume in the Yangtze basin that includes Danjiangkou reservoir (1960s), Gezhouba (1980s), and TGR (2003) (Table 1).

The DISC-SILICON module simulates the pelagic (PHYP_Si_Pelagic) and benthic diatoms (PHYP_Si_Benthic) and pelagic (Det_Si_Pelagic) and benthic detritus silicon (Det_Si_Benthic) by coupling hydrological parameters, temperature, and solar radiation (Figure 1). DSi inputs to the model occur via rock weathering and sewage wastewater discharge. Det_Si includes allochthonous (phytoliths from soil erosion) and autochthonous (mortality of PHYP_Si_Pelagic) materials. BSi is the sum of pelagic and benthic PHYP_Si and Det_Si. Physical dynamics of Det_Si are controlled by sedimentation and erosion equations which are linked to particulate inorganic matter (PIM), mostly sediment.

In general terms, DISC-SILICON dynamically computes various Si pools (denoted with capital *P*) and flows (capital *F*) for each stream, river, lake, and reservoir from headwaters to the coast along the river continuum (Figure 1). For every time

https://dx.doi.org/10.1021/acs.est.0c01465
Environ. Sci. Technol. 2020, 54, 11940−11950

Table 1. Source of Input and Validation Data

parameter/data type	data source
	Hydrology
runoff, water area and volume, discharge, and flow direction for1900−2010	PCR-GLOBWB[47,48]
reservoirs	Date of construction, area, depth, and volume for 6862 dams in the world[36]
lakes	global lakes and wetlands database (GLWD)[59]
	Meteorology
temperature	global climate database[60]
solar radiation	model describing irradiation as a function of latitude and turbidity[61]
	Diffuse Sources
soil loss and soil type	IMAGE-GNM[44]
lithology	global lithology map at 5 by 5 min resolution[62]
Det_Si content in soil	data from the Riverstrahler model[45]
	Point Source
population	IMAGE-GNM[44]
DSi and Det_Si waste water effluent	data from the Riverstrahler model[45]
	Water quality
validation data in Rhine	GLORICH database (https://www.geo.uni-hamburg.de/en/geologie/forschung/geochemie/glorich.html)[63]
validation data in Yangtze	Changjiang Water Resources Commission[38] from 1960 to 1984 and the literature[64,65] for the period after 1984

step, the change of a Si pool for species i in the grid cell c considered is calculated as follows

$$\frac{dP_{i,c}}{dt} = F_{up,i,c} + F_{inp,i,c} - F_{out,i,c} + \sum_{n}^{Num} F_{n,c} \quad (1)$$

where $F_{up,i,c}$ is the input flux [Mmol yr^{-1}] of Si species i from upstream grid cells to grid cell c. $F_{inp,i,c}$ is the input flux [Mmol yr^{-1}] from within grid cell c and $F_{out,i,c}$ is the output flux [Mmol yr^{-1}] from grid cell c to a neighboring grid cell downstream. $F_{n,c}$ (Mmol yr^{-1}) is the transformation flux from one Si species to another one within grid cell c as a result of in-stream biogeochemical processing (see Figure 1 and Table 2) and Num is the total number of fluxes (see Figure 1 and Table 2). $F_{n,c}$ is positive, when it enters pool $P_{i,c}$; it is negative, when it leaves pool $P_{i,c}$. The benthic species are not transported to downstream (i.e., $F_{up,i,c} = 0$ and $F_{out,i,c} = 0$).

Section 2.2 discusses the inputs ($F_{inp,i,c}$) of DSi and Det_Si to surface water, and the in-stream Si biogeochemical Si fluxes ($F_{n,c}$) are presented in Section 2.1.3. The data used to drive DISC-SILICON are listed in Table 1.

2.1.2. Si Delivery to Water Bodies. The DSi weathering fluxes F_1 and F_2 (Figure 1) are based on the model presented by Hartmann et al.[49] We added the impact of land use on silicon biogeochemistry, represented by a factor based on Struyf et al.[9] for 52 Scheldt sub-basins (see details in the Supporting Information 1).

The detritus Si input flux ($F_{inp,soil\_Det\_Si}$) representing soil erosion loss (Figure 1) is based on the approach of Cerdan et al.,[50] considering soil texture, land cover, and slope.[44] The land-use specific soil loss rates for the fractions of natural ecosystems, grassland, and arable land area were applied to every grid cell. The soil loss input to the river is in the form of PIM, and Si is a fraction of PIM based on the observed Si content in arable soil samples in the Seine river basin (4.9 mg

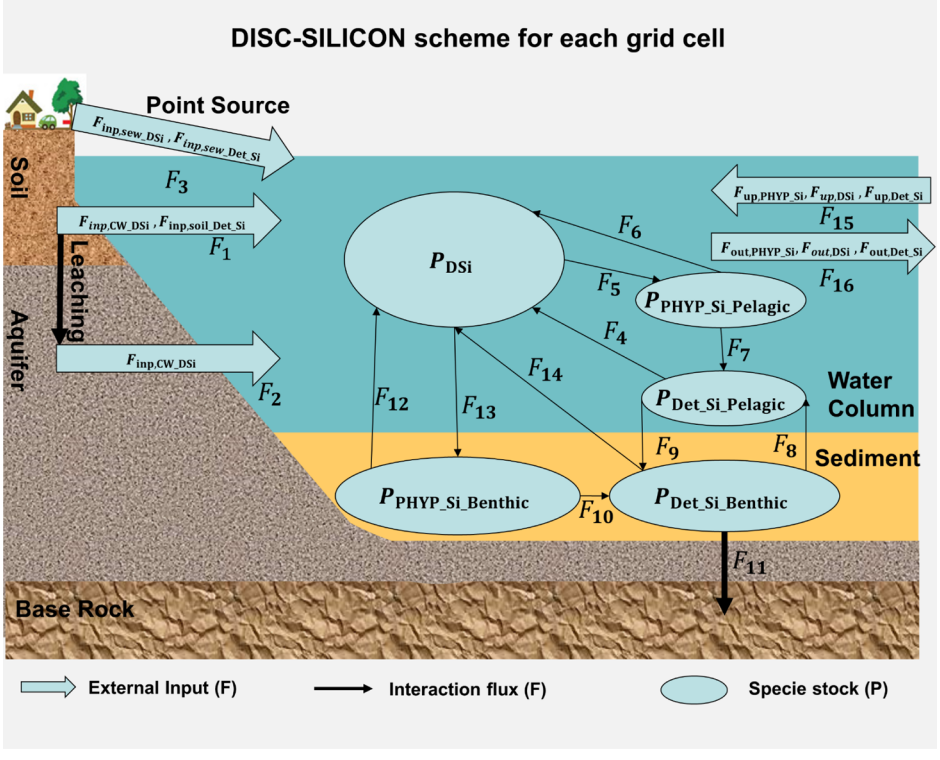

Figure 1. Scheme of the DISC-SILICON module showing the external input fluxes (F_1−F_3), the transformation fluxes F_4−F_{16} between the pools P_{DSi}, $P_{PHYP\_Si\_Pelagic}$, and P_{Det_Si} in the water column and $P_{PHYP\_Si\_Benthic}$ and $P_{Det\_Si\_Benthic}$ in the sediment within each grid cell, and the transfers with neighboring grid cells. The numbers correspond to the fluxes listed in Table 2.

https://dx.doi.org/10.1021/acs.est.0c01465
Environ. Sci. Technol. 2020, 54, 11940−11950

Table 2. List of Processes and Equations in Each Grid Cell[a]

flux #	description
F_1	Det_Si input from soil particles into the water (erosion) DSi input from weathering via surface runoff
F_2	DSi input from weathering via ground water
F_3	DSi input from the point source Det_Si input from the point source
F_4	Det_Si_Pelagic dissolution which is dependent on water temperature, the dissolution rate, and size of the pool of the Det_Si_Pelagic. $f(T_W)*k_{max\_Det\_Si\_Pelagic\_dissolution}*P_{Det\_Si\_Pelagic}$ where T_W(°C) is the water temperature and $f(T_W) = e^{-(T_{opt,growth}-T)^2/(T_{sigma,growth})^2}$
F_5 and F_{13}	PP (diatom growth) $k_{max\_growth}*Lim_{light}*f(T_W)*DSi_{conc}/(K_{DSi,PP} + DSi_{conc})$ where k_{max_growth} is the maximum diatom growth rate which differs between pelagic and benthic diatoms. DSi_{conc} is the DSi concentration in the water column and $K_{DSi,PP}$ is the half saturation concentration in the Michaelis–Menten function. The light intensity limitation is calculated both for pelagic and benthic diatoms, using the spatial distribution of solar radiation and light attenuation with depth using turbidity of the water column. Lim_{light} is the light limitation which is calculated using solar radiation and water turbidity. $Lim_{light} = \frac{I_z(lat)}{(I_z(lat) + k_{I,PHYP,Si,Benthic})}$, for benthic diatoms $Lim_{light} = \frac{\int_0^z I_0(lat)}{\left(\int_0^z I_0(lat) + k_{I,PHYP,Si,Pelagic}\right)}$, for pelagic diatoms where I_z and z are light intensity and depth, respectively, k_I is the half saturation for light limitation with the Michaelis–Menten equation; here, we use the Beer-Lambert equation. $I_z = I_0(lat)*e^{-\eta_{tot}*z}$ where $I_{0(lat)}$ is the solar radiation on the water surface at latitude lat, $I_0(lat) = \theta s(lat)*I_{solar\_constant}$ θs is the solar zenith angle, $I_{solar\_constant}$ is the solar constant 1367 $Wm^{-2.}$ η_{tot} is the water turbidity which is calculated with all the particulate matter that affect the light attenuation: $\eta_{tot} = \eta_{water} + \eta_{Det\_Si}*[P_{Det\_Si\_Pelagic}] + \eta_{PHYP\_Si\_Pelagic}*[P_{PHYP\_Si\_Pelagic}] + \eta_{PIM}*[P_{PIM}]$ where P_{PIM} is the total PIM, mostly is sediment.
F_6 and F_{12}	sum of DSi from diatom respiration and diatom excretion. diatom respiration: $f(T_W)*k_{resp}*P_{PHYP\_Si\_Pelagic/Benthic}$ diatom excretion: $f(T_W)*k_{excr}*P_{PHYP\_Si\_Pelagic/Benthic}$
F_7 and F_{10}	Det_Si_Pelatic/Benthic from diatom mortality $f(T_W)*k_{lysis}*(1 + \alpha*(1 + V_f))P_{PHYP\_Si\_Pelagic/Benthic}$ where α is 1 (if $P_{PHYP\_Si\_Pelagic/Benthic} > PHYP\_Si_{lim\_pelagic/benthic}$ or $T > 15$ °C), otherwise α is 0
F_8	the erosion of Det_Si_Benthic is a fraction of the total erosion ΦERO_{tot}[ton yr^{-1}]. $ERO_{Det.Si.Benthic} = \frac{P_{Det.Si.Benthic}}{P_{tot,sed}}*ERO_{tot}$ where $P_{Det\_Si\_Benthic}$ is the benthic Det_Si pool. Total erosion is calculated according to: $ERO_{tot} = k_{ero}*(P_{tot\_sed}/Area)/(k_{sed} + P_{tot\_sed}/Area)*S*Area*v$ where k_{ero} is the erosion coefficient, k_{sed} is the half-saturation constant, P_{tot_sed} is the total mass of sediment in the water body, S is the slope, Area is the bedarea, and v is the flow velocity. The total sedimentation is the sum of benthic PIM and benthic Det_Si: $P_{tot\_sed} = P_{PIM\_Benthic} + P_{Det\_Si\_Benthic}$
F_9	sedimentation of detritus silicon from the pelagic to the benthic pool. $V_{sed,Det\_Si\_Pelagic}/Depth*P_{Det\_Si\_Pelagic}$
F_{11}	burial of Det_Si_Benthic $burial = MIN\left(0 \text{ if } SED < SED_{lim},\ k_{burial.max}*\frac{SED - SED_{lim}}{SED}\right)$ where k_{burial_max} is the maximum burial rate, SED is the deposited PIM and $P_{Det\_Si\_Pelagic}$, and SED_{lim} is the threshold sediment stock. Burial occurs when $SED > SED_{lim}$.
F_{14}	dissolved silica flux from the Det_Si_Benthic pool in the upper sediment layer to the P_{DSi} pool. We assume no DSi production from buried Det_Si. $F_{Det\_Si\_Benthic\_dissolution} = -f_{Si}*P_{Det\_Si\_Benthic}*k_{max\_Det\_Si\_Benthic\_dissolution}$ where Det_Si_Benthic is the detritus Si in the upper sediment layer. $f_{Si} = [1 - Det\_Si\_Benthic/(Det\_Si\_Benthic + \exp(0.08*T_W))] - (0.3 + 0.02*T_W)*DSi_{conc}/28$ where DSi_{conc} is the DSi concentration, T_W is the water temperature.
F_{15}	input flux from upstream grid cell
F_{16}	output flux to downstream grid cell

[a]All parameters and values including units are presented in Supporting Information 3.

https://dx.doi.org/10.1021/acs.est.0c01465
Environ. Sci. Technol. 2020, 54, 11940–11950

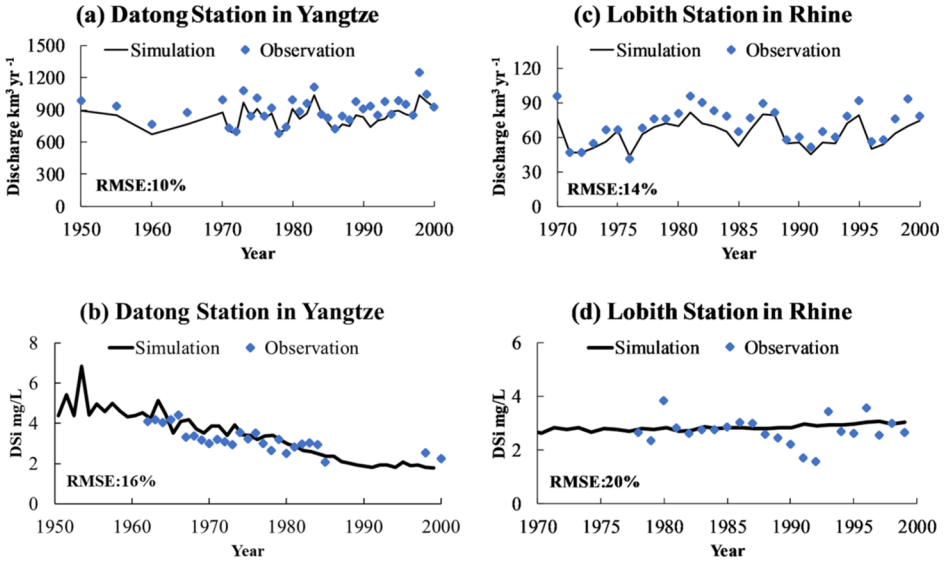

Figure 2. Comparison of measured and modeled discharge and DSi (Si) concentrations in the station of Datong in Yangtze (a,b) and Lobith in Rhine (c,d). The sources of the measurement data are listed in Table 1.

Det_Si Si/g soil, with a range of 2.5−7.3[45]). Here, an average fraction of 4.9 mg Si/g is multiplied with PIM to calculate the Det_Si input from soil loss.

The Si input flux F_3 (Figure 1) from the sewage water effluent ($F_{inp,sew\_Det\_Si} + F_{inp,sew\_DSi}$) is assumed to be 1.0 g Si per capita per day,[45] and the total input per grid cell is obtained by multiplying with the number of inhabitants within the grid cell ($N_{population}$) (Table 1). The Det_Si fraction of total Si in wastewater is assumed to be 25%, the complement (75%) being in the form of DSi.

$$F_{inp,sew.Det.Si} = r_{sew.Det.Si} * N_{population} \quad (2)$$

$$F_{inp,sew_{DSi},c} = r_{sew.DSi} * N_{population,c} \quad (3)$$

where $r_{sew\_Det\_Si}$ and r_{sew_DSi} are the specific Si loads per inhabitant which equals 0.75 g and 0.25 g Si per capita per day, respectively.

2.1.3. In-Stream Si Cycling. In the water column, DISC-SILICON includes 5 Si pools and 16 process fluxes (Figure 1, Table 2). As the model describes processes generically for different water bodies, DISC-SILICON allows us to assess the impact of external drivers (land use change, sewage source, weathering, climate, and hydrology) on the Si biogeochemistry along the river continuum. We initialize the model with a spin-up period of 50 years to obtain the equilibrium state for the benthic pools.

The change in the DSi pool $P_{DSi,c}$ in the water column in grid cell c is computed for each time step. DSi in the water column can be taken up by diatom growth (PHYP_Si_Pelagic growth and PHYP_Si_Benthic growth) (Figure 1, Table 2, #5 and 13). DSi is released by decomposition and dissolution from the pelagic and benthic detritus (Det_Si_Pelagic and Det_Si_-Benthic). The degradation rate for pelagic detritus is temperature-dependent. Det_Si_Benthic is transferred to pelagic DSi across the sediment−water interface, according to the empirical relationship presented by Billen et al.[51] (Figure 1, Table 2, #14).

The pools $P_{PHYP\_Si\_Pelagic,c}$ and $P_{PHYP\_Si\_Benth,c}$ are the Si pools in pelagic and benthic diatoms, respectively, in grid cell c. Benthic diatoms are the primary consumers of DSi in shallow water bodies.[52−54] With the variation of temperature, turbidity, depth, and light attenuation, DISC-SILICON simulates the growth of diatoms in every water body and grid cell (Figure 1, Table 2, #5 and #13). Pelagic and benthic diatoms are transformed into Det_Si_Pelagic and Det_Si_Benthic using diatom mortality (Figure 1, Table2, #7 and #10). The Det_Si_Pelagic and Det_Si_Benthic are linked by in-stream sedimentation and resuspention (Figure 1, Table 2, #9 and #8). Det_Si_Benthic can be removed by burial in the sediment, which occurs when the accumulated bed sediments (total mass) exceed 500 g/m^2 (Figure 1, Table 2, #11).

2.2. Sensitivity Analysis. We have deliberately not calibrated our model. Instead, to investigate model performance and model defects, we analyzed the sensitivity of the export of all forms of Si to the ocean and the diatom production in the water column (pelagic diatom PP; PP_PHYP_Si_Pelagic = F_5 in Figure 1) to changes in 53 model parameters using Latin hypercube sampling.[55] We executed 750 runs to calculate the sensitivity for the period 1996−2000 for both the rivers Rhine and Yangtze. The standardized regression coefficient (SRC, more details are provided in Supporting Information 2) is used as an indicator of the relative influence of a model parameter on model results (export of Si to the ocean and diatom production). Parameters are considered to be important if their influence on the model result exceeds 4% (i.e., SRC < −0.2 or SRC > 0.2; see Supporting Information 4).

3. RESULTS AND DISCUSSION

3.1. Comparison with Measurement Data and Sensitivity Analysis. The model results show a good agreement with the observed data both for the Datong station in the Yangtze (Figure 2a,b) and Lobith in the Rhine (Figure 2c,d) for the period 1960−2000. The root mean squared error (RMSE, more details in Supporting Information 2) for the discharge and DSi concentration are 10% and 16%, respectively, for the Datong station in the Yangtze. The model reproduces the trend of DSi during the period 1960s−1980s (Figure 2b). The RMSEs for the discharge and DSi concentration are 14% and 20%, respectively, for the Lobith

https://dx.doi.org/10.1021/acs.est.0c01465
Environ. Sci. Technol. 2020, 54, 11940−11950

Table 3. SRC Representing the Relative Sensitivity of the Model Performance for 3 Output Parameters [Dissolved Si Export to Mouth (DSi_Export), Phytoplankton Si and Detritus Si Export to Mouth (BSi_Export), and Pelagic Diatom PP (PP_PHYP_Si_pelagic, F5 in Figure 1)] for the Rhine and Yangtze River to the Variations of 53 Model Input Parameters[a]

	Rhine			Yangtze		
parameters	DSi_export	BSi_export	PP_PHYP_Si_Pelagic	DSi_Export	BSi_Export	PP_PHYP_Si_Pelagic
solar_radiation	−0.10	0.14	0.18	−0.14	0.27	0.22
temperature	0.03	−0.08	0.55	0.17	−0.19	0.19
slope	0.02	0.23	−0.01			
discharge	0.02	0.66	−0.05		0.50	−0.07
$T_{opt\_Det\_Si\_Benthic\_dissolution}$			−0.02	−0.20	0.31	−0.02
$k_{I,PHYP\_Si\_Pelagic}$	0.02	−0.03		0.10	−0.18	−0.24
$T_{opt\_Det\_Si\_Benthic\_dissolution}$	−0.12	0.22				
$V_{sed,Det\_Si\_Pelagic}$		−0.34		−0.08	−0.26	−0.01
T_{opt_growth}	0.08	−0.10	−0.50			
$T_{sigma\_Det\_Si\_Pelagic\_menera}$	−0.04	0.05	0.23			
$k_{max\_growth\_pelagic}$	−0.06	0.09	0.32	−0.20	0.35	0.47
$PHYP\_Si_{lim\_pelagic}$	−0.05	0.10	0.28	−0.15	0.33	0.45
PIMload2river	−0.02	−0.22				
F_{inp,CW_DSi}	0.97	0.03	0.02	0.76	0.06	0.08

[a]The complete results of the sensitivity analysis are presented in Supporting Information 4. Values without color indicate −0.2 < SRC < 0.2; values with green and salmon colors indicate values <−0.2 and >0.2, respectively Positive values indicate that a higher input parameter value generates a higher model output variable, and negative values indicate that a higher input parameter value generates a lower model output variable.

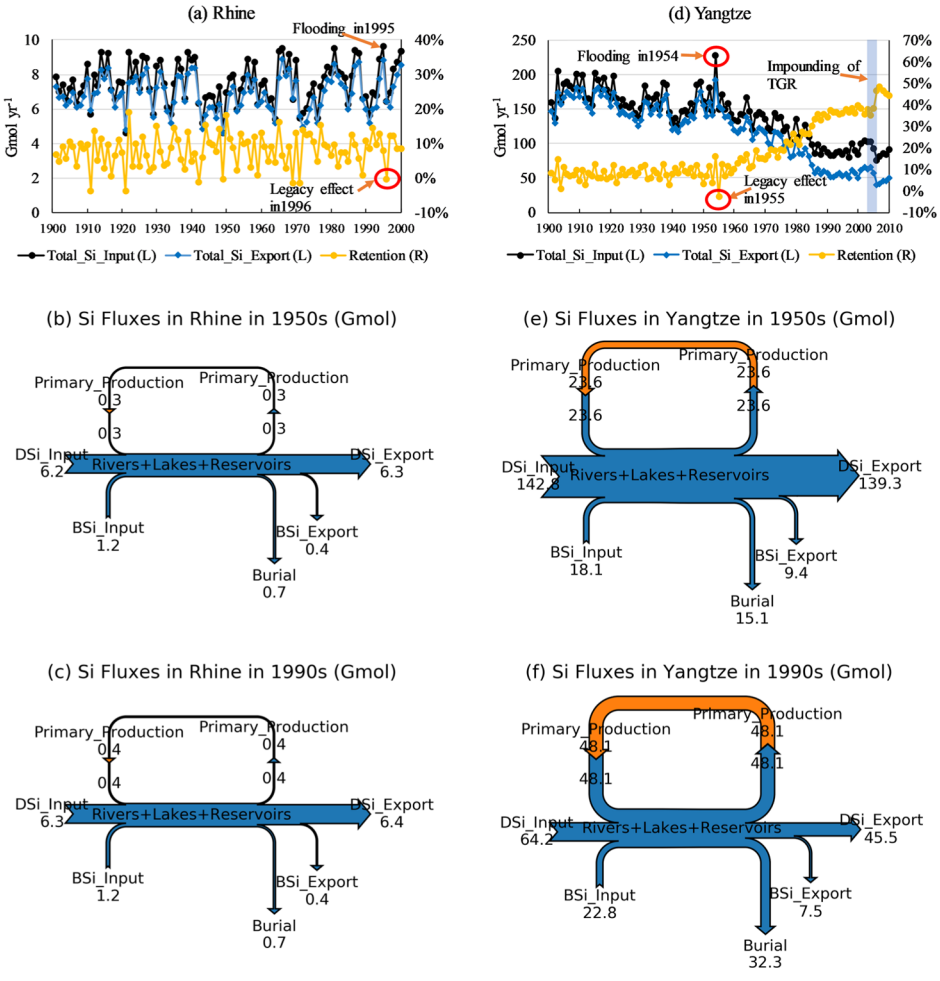

Figure 3. Total Si input into the river and the export to the river mouth (left *y*-axis) and retention in percentage (right *y*-axis) in the Rhine (a) and Yangtze (d). Annual average DSi and BSi (Det_Si_Pelagic + PHYP_Si_Pelagic) budget for the Rhine (b,c) and Yangtze (e,f) in the 1950s and 1990s. All fluxes are expressed in Gmol yr^{-1}.

https://dx.doi.org/10.1021/acs.est.0c01465
Environ. Sci. Technol. 2020, 54, 11940−11950

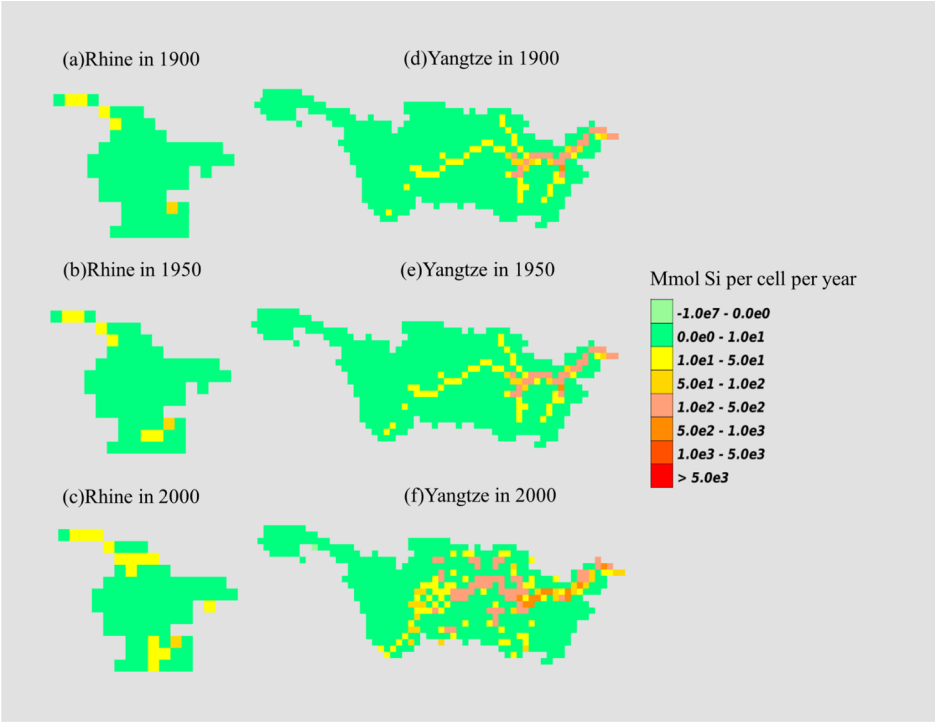

Figure 4. Spatial distribution of diatom PP in the Rhine (a−c) and the Yangtze (d−f) in 1900, 1950, and 2000. Movie SI4 shows the yearly diatom PP during the period 1900−2010 (for Rhine 1900−2000).

station in the Rhine. Considering that DISC-SILICON is a global model based on global data and parameter settings, the agreement with the available observations is satisfactory based on general model performance criteria.[56]

The full list of input parameters which have a significant effect on the model output is provided in Supporting Information 4. Here, the focus is on DSi and BSi export to the river mouth and pelagic diatom PP (Table 3). Both in Rhine and Yangtze, the DSi_Export is strongly controlled by DSi_Input from weathering. The SRCs for DSi_Export in the Yangze (0.76) and Rhine (0.97) are both much higher than values for other model parameters. For the Yangtze, the optimal temperature for the benthic dissolution process influences the DSi_Export, in contrast to the Rhine. This is because instream processes are playing a much more important role in the Yangtze than in the Rhine because of the much longer average travel time: 0.19 and 0.04 yr in 2000 for the Yangtze and Rhine, respectively.

The BSi_Export from the Yangtze basin is negatively influenced by the detritus settling velocity for waterbodies. In contrast, there is a positive effect of solar radiation, discharge, optimal temperature for dissolution, the maximum growth rate for pelagic diatoms, and the threshold concentration for mortality of diatoms. Compared with the Yangtze, the BSi_Export in the Rhine basin is sensitive to the slope and PIM. The difference between the Rhine basin and Yangtze basin is caused by the absence of major reservoirs in the Rhine basin, causing the average travel time of water to be much shorter than that in the Yangtze. For pelagic diatom PP, the results of the sensitivity analysis show that solar radiation, half saturation of light limitation, maximum growth rate, threshold concentration for mortality, and the mortality rate are important parameters.

The sensitivity analysis indicated that the modeled Si export and diatom PP are sensitive to DSi input from weathering, growth factors (growth rate and mortality rate of diatoms, temperature, and solar radiation), and factors related to the travel time of water (discharge, slope, and water body width and depth). These factors and the growth and mortality rates of diatoms require further attention, for example, by involving mechanistic knowledge from other disciplines (hydrology and biology) in model development.

3.2. Si Input, Export, and Retention. To compare the two rivers, we aggregated the total Si input fluxes to the Rhine and Yangtze networks. The total Si delivery and export for the Rhine show interannual variation but lack a trend for the period 1900−2000 (Figure 3a); the retention (calculated as the difference between Si inputs and exports divided by Si inputs) varied between −4% and 19% (average 8%) (Figure 3a). For the Yangtze basin, we see a different pattern, with total annual Si delivery varying between 128 and 205 Gmol yr^{-1} between 1900 and 1950, followed by a sharp decrease from 161 to 85 Gmol yr^{-1} during 1950−2000 (Figure 3d). This decline is mainly due to land use changes. Since 1950, around 40% of the area covered by natural ecosystems has been transformed to cropland, and thus, Si inputs from terrestrial sources have declined significantly. In the first half of the 20th century, the retention in the Yangtze varied between −0.7% and 13% (average 6%) (Figure 3d). After 1950, the retention rapidly increased to 29% in 2000 (Figure 3d) because of construction of reservoirs and Si input decrease.

The DISC-SILICON model properly reproduces the impact of extremely wet years, such as 1995 in the Rhine and 1954 and 1998 in the Yangtze. In such wet years, the model simulates a significant increase in total Si and Det_Si inputs; part of the enhanced DSi is transformed into diatom biomass and accumulates in the benthos. The model results point to a

https://dx.doi.org/10.1021/acs.est.0c01465
Environ. Sci. Technol. 2020, 54, 11940−11950

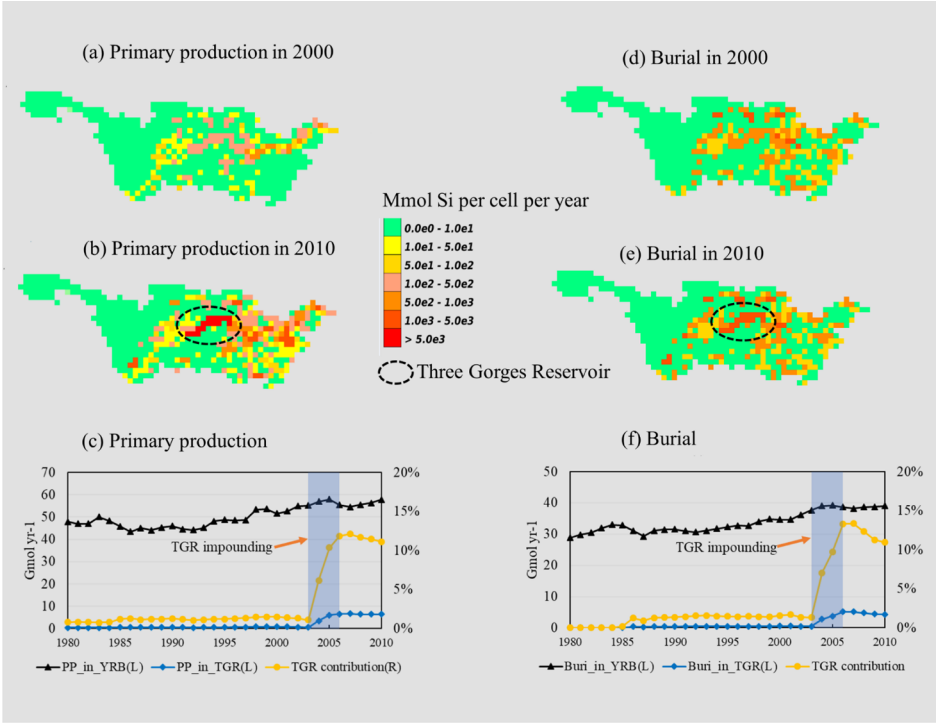

Figure 5. Spatial distribution of diatom PP before (a) and after (b) the TGR impounding in Yangtze and (c) diatom PP in the TGR and YRB and TGR contribution to YRB. Spatial distribution of burial in the Yangtze before (d) and after (e) the TGR impounding and (f) burial in TGR and YRB and TGR contribution to YRB. Blue bar (c,f) indicates the TGR impounding years.

legacy (red circle in Figure 3a,d), especially when a wet year is followed by a dry year (for instance, 1996 in the Rhine and 1955 in the Yangtze), and the Si retention then even becomes negative as a result of DSi release from Det_Si_Benthic.

The average DSi and BSi budget for the 1950s and 1990s for the Rhine river show no obvious trend. However, for Yangtze, the DSi input showed a dramatic decrease from the 1950s to 1990s of 143 to 64 Gmol yr^{-1}, while the BSi input increased from 18 to 23 Gmol yr^{-1} (Figure 3e,f). Because of the construction of dams, the pelagic diatom PP increased from 24 to 48 Gmol yr^{-1}, burial of detritus increased from 15 to 32 Gmol yr^{-1}, and DSi_Export decreased from 139 to 46 Gmol yr^{-1} from the 1950s to the 1990s.

Although the Rhine river shows no trend for the export flux of Si, the Si export to the East China and Yellow Seas from the Yangtze has been rapidly declining since the second half of the 20th century as a result of dramatic changes in land use affecting the Si supply from weathering and erosion and dam construction affecting the burial of biogenic silica. This has been shown to lead to changes in the ecology of the reservoirs (Figure 4), and together with nutrient loading and changing, stoichiometry has dramatic impacts in Chinese coastal marine ecosystems including HABs.[19,25−27,57]

3.3. Spatial and Temporal Distribution of PP by Diatoms. Our results indicate that there is important spatial variation in diatom production and, hence, Si uptake. Furthermore, significant changes in the production have taken place during the course of the 20th century. DISC-SILICON simulates an almost twofold increase in diatom PP during the period 1900−2000 in the Rhine basin (Figures 3b,c and S3), with hotspots in the lower reach and Lake Constance (Figure 4a−c). In contrast, the Yangtze basin has been increasingly perturbed by reservoirs (Figure S3). The pelagic diatom PP in the Yangtze basin varied between 18 and 22 Gmol yr^{-1} (average 21 Gmol yr^{-1}) during the first half of the 20th century but increased rapidly to 52 Gmol yr^{-1} (Figure 3e,f) in 2000 because of the dam construction and increasing reservoir volume, which favored diatom growth (Figure 5a−c) and settling of BSi in the sediments of reservoirs. In both basins, the increase in diatom PP by diatoms occurs especially in the middle and lower reaches (Figure 4−f).

3.4. Impact of the TGR. Our simulations show that total Si retention (Figure 3d) in the Yangtze River basin (YRB) increased from 38% (average for 1999−2002) to 46% (average for 2007−2010). This retention increase is mainly due to the impounding of the TGR between 2003 and 2006. The contribution of the TGR to the whole-basin diatom PP increased from 1% (average for 1999−2002) to 12% (average for 2007−2010) (Figure 5a−c), which also caused an increase in the Det_Si_Plegic and Det_Si_Benthic pools. The contribution of the TGR to the whole-basin burial increased from 2% (average for 1999−2002) to 12% (average for 2007−2010) (Figure 5d−f). In addition to the land-use impact on the weathering supply of Si, the enhanced retention in the TGR further reduces the Si export to the mouth, with two major consequences. Enhanced retention within the reservoir may have severe consequences for downstream ecosystems, for example, a shift from diatoms to green algae in the lower river or the proliferation of harmful algae in the coastal ocean.[8,58] DISC-SILICON estimates for retention in the TGR are in agreement with the estimated 6% retention of reactive dissolved and particulate Si.[13]

3.5. Model Limitations and Future Improvements. Construction of a large number of dams is planned in the Yangtze river and many other rivers.[36] IMAGE-DGNM will be a helpful tool to project future changes in Si cycling and river Si export to the global coastal ocean under scenarios of climate change and human disturbances. IMAGE-DGNM including

https://dx.doi.org/10.1021/acs.est.0c01465
Environ. Sci. Technol. 2020, 54, 11940−11950

DISC-SILICON is the first model that allows us to describe the long-term spatial patterns of global Si transport and biogeochemical processing in the river continuum (from bed rock weathering, soil to streams, from upstream to downstream, lakes and reservoirs). The model reproduces observed Si concentrations, the effect of dam construction and enhanced retention in reservoirs, the effect of land use changes on the delivery of Si, and the effect of climate variability. The spatial variation of diatom production and uptake, decay of diatom biomass, dissolution of BSi, and the changes in the course of the 20th century highlight the need for a spatially explicit model. However, the model has limitations that need attention in future model improvements.

The DSi input from weathering clearly depends on the Si biogeochemical cycling in soils. Because our approach for describing the impact of land use on the weathering supply of Si is nonspatial (lumped for the whole river basin), future model improvements should focus on the improvement of the description of the Si transformation in the soil-plant system (crop harvest) at the grid cell scale and the subsequent transport via shallow and deep groundwater. A further limitation of the model is a lack of coupling of the Si to carbon and the other nutrients. Such a coupling will lead to a better description of the Si cycle in rivers accounting for the changes in N and P biogeochemistry.

■ ASSOCIATED CONTENT

Supporting Information

The Supporting Information is available free of charge at https://pubs.acs.org/doi/10.1021/acs.est.0c01465.

Model description (PDF)

Spatially explicit changes of diatom PP in Rhine for the period 1900−2000 and Yangtze for the period 1900−2010 (ZIP)

■ AUTHOR INFORMATION

Corresponding Author

Xiaochen Liu − *Department of Earth Sciences, Faculty of Geosciences, Utrecht University, 3584 CB Utrecht, The Netherlands;* orcid.org/0000-0003-2973-8132; Email: x.liu@uu.nl

Authors

Wim Joost van Hoek − *Department of Earth Sciences, Faculty of Geosciences, Utrecht University, 3584 CB Utrecht, The Netherlands*

Lauriane Vilmin − *Deltares, 2600 MH Delft, The Netherlands*

Arthur Beusen − *Department of Earth Sciences, Faculty of Geosciences, Utrecht University, 3584 CB Utrecht, The Netherlands; PBL Netherlands Environmental Assessment Agency, 2500 GH The Hague, The Netherlands*

José M. Mogollón − *Institute of Environmental Sciences (CML), Leiden University, 2300 RA Leiden, The Netherlands*

Jack J. Middelburg − *Department of Earth Sciences, Faculty of Geosciences, Utrecht University, 3584 CB Utrecht, The Netherlands;* orcid.org/0000-0003-3601-9072

Alexander F. Bouwman − *Department of Earth Sciences, Faculty of Geosciences, Utrecht University, 3584 CB Utrecht, The Netherlands; PBL Netherlands Environmental Assessment Agency, 2500 GH The Hague, The Netherlands; Laboratory of Marine Chemistry Theory and Technology, Ministry of Education, Ocean University of China, Qingdao 266100, PR China;* orcid.org/0000-0002-2045-1859

Complete contact information is available at: https://pubs.acs.org/10.1021/acs.est.0c01465

Author Contributions

X.L. wrote the original draft and developed the DISC-SILICON module with W.J.v.H., and L.V. A. H. W. B., A.F.B., and J.M.M. developed the IMAGE-DGNM framework. A.F.B. and J.J.M. contributed to the research objectives and model concept. All the coauthors contributed to writing the text.

Notes

The authors declare no competing financial interest.

■ ACKNOWLEDGMENTS

A.F.B. and A.B. received support from PBL Netherlands Environmental Assessment Agency through in-kind contributions to The New Delta 2014 ALW project nos. 869.15.015 and 869.15.014. Jack Middelburg was supported by the Netherlands Earth System Science Center.

■ REFERENCES

(1) Berner, E.; Berner, R. Global Environment: Water, Air, and Geochemical Cycles. *Choice Rev.* **1996**, *33*, 33.

(2) Tréguer, P. J.; De La Rocha, C. L. The world ocean silica cycle. *Annu. Rev. Mar. Sci.* **2013**, *5*, 477−501.

(3) Treguer, P.; Nelson, D. M.; Van Bennekom, A. J.; DeMaster, D. J.; Leynaert, A.; Queguiner, B. The silica balance in the world ocean: a reestimate. *Science* **1995**, *268*, 375−379.

(4) Conley, D. J. Biogeochemical nutrient cycles and nutrient management strategies. *Hydrobiologia* **1999**, *410*, 87−96.

(5) Conley, D. J. Terrestrial ecosystems and the global biogeochemical silica cycle. *Global Biogeochem. Cycles* **2002**, *16*, 68−71.

(6) Derry, L. A.; Kurtz, A. C.; Ziegler, K.; Chadwick, O. A. Biological control of terrestrial silica cycling and export fluxes to watersheds. *Nature* **2005**, *433*, 728.

(7) Tavernini, S.; Pierobon, E.; Viaroli, P. Physical factors and dissolved reactive silica affect phytoplankton community structure and dynamics in a lowland eutrophic river (Po river, Italy). *Hydrobiologia* **2011**, *669*, 213−225.

(8) Garnier, J.; Beusen, A.; Thieu, V.; Billen, G.; Bouwman, L., N: P: Si nutrient export ratios and ecological consequences in coastal seas evaluated by the ICEP approach. *Global Biogeochem. Cycles* **2010**, *24*, (). DOI: 10.1029/2009gb003583

(9) Struyf, E.; Smis, A.; Van Damme, S.; Garnier, J.; Govers, G.; Van Wesemael, B.; Conley, D. J.; Batelaan, O.; Frot, E.; Clymans, W.; Vandevenne, F.; Lancelot, C.; Goos, P.; Meire, P. Historical land use change has lowered terrestrial silica mobilization. *Nat. Commun.* **2010**, *1*, 129.

(10) Phillips, A. K.; Cowling, S. A. Biotic and abiotic controls on watershed Si cycling and river Si yield in western Canada. *Biogeochemistry* **2019**, *143*, 221−237.

(11) Kelly, E. F.; Chadwick, O. A.; Hilinski, T. E. The effect of plants on mineral weathering. *Biogeochemistry* **1998**, *42*, 21−53.

(12) Humborg, C.; Blomqvist, S.; Avsan, E.; Bergensund, Y.; Smedberg, E.; Brink, J.; Mörth, C.-M. Hydrological alterations with river damming in northern Sweden: Implications for weathering and river biogeochemistry. *Global Biogeochem. Cycles* **2002**, *16*, 12.

(13) Maavara, T.; Dürr, H. H.; Van Cappellen, P. Worldwide retention of nutrient silicon by river damming: From sparse data set to global estimate. *Global Biogeochem. Cycles* **2014**, *28*, 842−855.

(14) Harrison, J. A.; Frings, P. J.; Beusen, A. H. W.; Conley, D. J.; McCrackin, M. L., Global importance, patterns, and controls of

dissolved silica retention in lakes and reservoirs. *Global Biogeochem. Cycles* **2012**, *26*, (). DOI: 10.1029/2011gb004228
(15) Ran, X.; Yu, Z.; Yao, Q.; Chen, H.; Guo, H. Silica retention in the Three Gorges Reservoir. *Biogeochemistry* **2013**, *112*, 209−228.
(16) Beusen, A. H. W.; Bouwman, A. F.; Dürr, H. H.; Dekkers, A. L. M.; Hartmann, J., Global patterns of dissolved silica export to the coastal zone: Results from a spatially explicit global model. *Global Biogeochem. Cycles* **2009**, *23*, (),. DOI: 10.1029/2008gb003281
(17) Jossette, G.; Leporcq, B.; Sanchez, N. Biogeochemical mass-balances (C, N, P, Si) in three large reservoirs of the Seine Basin (France). *Biogeochemistry* **1999**, *47*, 119−146.
(18) Humborg, C.; Pastuszak, M.; Aigars, J.; Siegmund, H.; Mörth, C.-M.; Ittekkot, V. Decreased silica land-sea fluxes through damming in the Baltic Sea catchment - Significance of particle trapping and hydrological alterations. *Biogeochemistry* **2006**, *77*, 265−281.
(19) Ran, X.; Bouwman, A. F.; Yu, Z.; Liu, J. Implications of eutrophication for biogeochemical processes in the Three Gorges Reservoir, China. *Reg. Environ. Change* **2019**, *19*, 55−63.
(20) Conley, D. J. Riverine contribution of biogenic silica to the oceanic silica budget. *Limnol. Oceanogr.* **1997**, *42*, 774−777.
(21) Wollheim, W. M.; Vörösmarty, C. J.; Bouwman, A. F.; Green, P.; Harrison, J.; Linder, E.; Peterson, B. J.; Seitzinger, S. P.; Syvitski, J. P. M., Global N removal by freshwater aquatic systems using a spatially distributed, within-basin approach. *Global Biogeochem. Cycles* **2008**, *22*, (). DOI: 10.1029/2007gb002963
(22) Billen, G.; Garnier, J.; Némery, J.; Sebilo, M.; Sferratore, A.; Barles, S.; Benoit, P.; Benoît, M. A long-term view of nutrient transfers through the Seine river continuum. *Sci. Total Environ.* **2007**, *375*, 80−97.
(23) Humborg, C.; Smedberg, E.; Medina, M. R.; Mörth, C.-M. Changes in dissolved silicate loads to the Baltic Sea - The effects of lakes and reservoirs. *J. Mar. Syst.* **2008**, *73*, 223−235.
(24) Anderson, D. M.; Glibert, P. M.; Burkholder, J. M. Harmful algal blooms and eutrophication: Nutrient sources, composition, and consequences. *Estuaries* **2002**, *25*, 704−726.
(25) Xiao, X.; Agustí, S.; Pan, Y.; Yu, Y.; Li, K.; Wu, J.; Duarte, C. M. Warming Amplifies the Frequency of Harmful Algal Blooms with Eutrophication in Chinese Coastal Waters. *Environ. Sci. Technol.* **2019**, *53*, 13031.
(26) Yu, R.-C.; Lü, S.-H.; Liang, Y.-B. Harmful algal blooms in the coastal waters of China. *Global Ecology and Oceanography of Harmful Algal Blooms*; Springer: 2018; pp 309−316.
(27) Zhou, M.; Shen, Z.; Yu, R. Responses of a Coastal Phytoplankton Community to Increased Nutrient Input from the Changjiang River. *Studies of the Biogeochemistry of Typical Estuaries and Bays in China*; Springer, 2020; pp 159−173.
(28) Clarke, F. W. *The Data of Geochemistry*; US Government Printing Office, 1920.
(29) Treguer, P.; Nelson, D. M.; Van Bennekom, A. J.; DeMaster, D. J.; Leynaert, A.; Quéguiner, B. The silica balance in the world ocean: a reestimate. *Science* **1995**, *268*, 375−379.
(30) Laruelle, G. G.; Roubeix, V.; Sferratore, A.; Brodherr, B.; Ciuffa, D.; Conley, D. J.; Dürr, H. H.; Garnier, J.; Lancelot, C.; LeThiPhuong, Q.; Meunier, J. D.; Meybeck, M.; Michalopoulos, P.; Moriceau, B.; Ni Longphuirt, S.; Loucaides, S.; Papush, L.; Presti, M.; Ragueneau, O.; Regnier, P.; Saccone, L.; Slomp, C. P.; Spiteri, C.; Van Cappellen, P., Anthropogenic perturbations of the silicon cycle at the global scale: Key role of the land-ocean transition. *Global Biogeochem. Cycles* **2009**, *23*, (). DOI: 10.1029/2008gb003267
(31) Dürr, H. H.; Meybeck, M.; Hartmann, J.; Laruelle, G. G.; Roubeix, V. Global spatial distribution of natural riverine silica inputs to the coastal zone. *Biogeosciences* **2011**, *8*, 597−620.
(32) Van Bennekom, A.; Salomons, W. Pathways of nutrients and organic matter from land to ocean through rivers. *Review and Workshop on River Inputs to Ocean Systems. Rome (Italy). 26 Mar 1979*, 1981.
(33) Humborg, C.; Ittekkot, V.; Cociasu, A.; Bodungen, B. V. Effect of Danube River dam on Black Sea biogeochemistry and ecosystem structure. *Nature* **1997**, *386*, 385−388.
(34) Humborg, C.; Conley, D. J.; Rahm, L.; Wulff, F.; Cociasu, A.; Ittekkot, V. Silicon retention in river basins: Far-reaching effects on biogeochemistry and aquatic food webs in coastal marine environments. *Ambio* **2000**, *29*, 45−50.
(35) Moon, S.; Chamberlain, C. P.; Hilley, G. E. New estimates of silicate weathering rates and their uncertainties in global rivers. *Geochim. Cosmochim. Acta* **2014**, *134*, 257−274.
(36) Lehner, B.; Liermann, C. R.; Revenga, C.; Vörösmarty, C.; Fekete, B.; Crouzet, P.; Döll, P.; Endejan, M.; Frenken, K.; Magome, J.; Nilsson, C.; Robertson, J. C.; Rödel, R.; Sindorf, N.; Wisser, D. High-resolution mapping of the world's reservoirs and dams for sustainable river-flow management. *Front. Ecol. Environ.* **2011**, *9*, 494−502.
(37) Vilmin, L.; Mogollón, J. M.; Beusen, A. H. W.; van Hoek, W. J.; Liu, X.; Middelburg, J. J.; Bouwman, A. F. Modeling process-based biogeochemical dynamics in surface freshwaters of large watersheds with the IMAGE-DGNM framework. *J. Adv. Model. Earth Syst.* **2020**, No. e2019MS001796.
(38) Changjiang River Water Resource Committee, Changjiang River Water Resource Committee, *Hydrographic Data Collection in the Lower Reaches of the Yangtze River (Internal Report)*; Changjiang Water Resources Commission, 1955−1985; p 585.
(39) Xing, G. X.; Zhu, Z. L. Regional nitrogen budgets for China and its major watersheds. *Biogeochemistry* **2002**, *57*, 405−427.
(40) Yan, W.; Zang, S.; Sun, P.; Seitzinger, S. P., How do nitrogen inputs to the Changjiang basin impact the Changjiang River nitrate: A temporal analysis for 1968-1997. *Global Biogeochem. Cycles* **2003**, *17*, (). DOI: 10.1029/2002gb002029
(41) Van der Weijden, C. H.; Middelburg, J. J. Hydrogeochemistry of the river Rhine: long term and seasonal variability, elemental budgets, base levels and pollution. *Water Res.* **1989**, *23*, 1247−1266.
(42) Tockner, K.; Uehlinger, U.; Robinson, C. T. *Rivers of Europe*; Academic Press, 2009.
(43) Admiraal, W.; Breugem, P.; Jacobs, D. M. L. H. A.; De Ruyter Van Steveninck, E. D. Fixation of dissolved silicate and sedimentation of biogenic silicate in the lower river Rhine during diatom blooms. *Biogeochemistry* **1990**, *9*, 175−185.
(44) Beusen, A. H. W.; Van Beek, L. P. H.; Bouwman, A. F.; Mogollón, J. M.; Middelburg, J. J. Coupling global models for hydrology and nutrient loading to simulate nitrogen and phosphorus retention in surface water − description of IMAGE−GNM and analysis of performance. *Geosci. Model Dev.* **2015**, *8*, 4045−4067.
(45) Sferratore, A.; Garnier, J.; Billen, G.; Conley, D. J.; Pinault, S. Diffuse and point sources of silica in the Seine River Watershed. *Environ. Sci. Technol.* **2006**, *40*, 6630−6635.
(46) Garnier, J.; d'Ayguesvives, A.; Billen, G.; Conley, D.; Sferratore, A. Silica dynamics in the hydrographic network of the Seine River. *Oceanis* **2002**, *28*, 487−508.
(47) Sutanudjaja, E. H.; Van Beek, R.; Wanders, N.; Wada, Y.; Bosmans, J. H. C.; Drost, N.; Van Der Ent, R. J.; De Graaf, I. E. M.; Hoch, J. M.; De Jong, K.; Karssenberg, D.; López López, P.; Peßenteiner, S.; Schmitz, O.; Straatsma, M. W.; Vannametee, E.; Wisser, D.; Bierkens, M. F. P. PCR-GLOBWB 2: A 5 arcmin global hydrological and water resources model. *Geosci. Model Dev.* **2018**, *11*, 2429−2453.
(48) Van Beek, L. P. H.; Wada, Y.; Bierkens, M. F. P. Global monthly water stress: 1. Water balance and water availability. *Water Resour. Res.* **2011**, *47*, W07517.
(49) Hartmann, J.; Moosdorf, N.; Lauerwald, R.; Hinderer, M.; West, A. J. Global chemical weathering and associated p-release - the role of lithology, temperature and soil properties. *Chem. Geol.* **2014**, *363*, 145−163.
(50) Cerdan, O.; Govers, G.; Le Bissonnais, Y.; Van Oost, K.; Poesen, J.; Saby, N.; Gobin, A.; Vacca, A.; Quinton, J.; Auerswald, K.; Klik, A.; Kwaad, F. J. P. M.; Raclot, D.; Ionita, I.; Rejman, J.; Rousseva, S.; Muxart, T.; Roxo, M. J.; Dostal, T. Rates and spatial variations of soil erosion in Europe: A study based on erosion plot data. *Geomorphology* **2010**, *122*, 167−177.

(51) Billen, G.; Garnier, J.; Silvestre, M. A simplified algorithm for calculating benthic nutrient fluxes in river systems. *Ann. Limnol.* **2015**, *51*, 37−47.
(52) Bowes, M. J.; Leach, D. V.; House, W. A. Seasonal nutrient dynamics in a chalk stream: The River Frome, Dorset, UK. *Sci. Total Environ.* **2005**, *336*, 225−241.
(53) House, W. A.; Leach, D. V.; Armitage, P. D. Study of dissolved silicon, and nitrate dynamics in a fresh water stream. *Water Res.* **2001**, *35*, 2749−2757.
(54) Leira, M.; Sabater, S. Diatom assemblages distribution in catalan rivers, NE Spain, in relation to chemical and physiographical factors. *Water Res.* **2005**, *39*, 73−82.
(55) Saltelli, A.; Chan, K.; Scott, E. M. *Sensitivity Analysis*; Wiley and Sons: Chichester, U.K., 2000.
(56) Moriasi, D. N.; Gitau, M. W.; Pai, N.; Daggupati, P. Hydrologic and water quality models: Performance measures and evaluation criteria. *Trans. ASABE* **2015**, *58*, 1763−1785.
(57) Glibert, P. M.; Berdalet, E.; Burford, M. A.; Pitcher, G. C.; Zhou, M. *Global Ecology and Oceanography of Harmful Algal Blooms*; Springer, 2018; Vol. *232*.
(58) Middelburg, J. J. Are nutrients retained by river damming? *Natl. Sci. Rev.* **2020**, DOI: 10.1093/nsr/nwaa073.
(59) Lehner, B.; Döll, P. Development and validation of a global database of lakes, reservoirs and wetlands. *J. Hydrol.* **2004**, *296*, 1−22.
(60) New, M.; Hulme, M.; Jones, P. Representing twentieth-century space-time climate variability. Part II: Development of 1901-96 monthly grids of terrestrial surface climate. *J. Clim.* **2000**, *13*, 2217−2238.
(61) van Hoek, W. J.; Vilmin, L.; Beusen, A. H. W.; Mogollón, J. M.; Liu, X.; Langeveld, J. J.; Bouwman, A. F.; Middelburg, J. J. CARBONDISC 1.0 - A coupled, process-based model of global in-stream carbon biogeochemistry. *Geosci. Model Dev. Discuss.* **2019**, *2019*, 1−31.
(62) Dürr, H. H.; Meybeck, M.; Dürr, S. H., Lithologic composition of the Earth's continental surfaces derived from a new digital map emphasizing riverine material transfer. *Global Biogeochem. Cycles* **2005**, *19*, (). DOI: 10.1029/2005gb002515
(63) Hartmann, J.; Lauerwald, R.; Moosdorf, N. A brief overview of the GLObal RIver CHemistry Database, GLORICH. *Procedia Earth Planet. Sci.* **2014**, *10*, 23−27.
(64) Wang, X.; Yang, S.; Ran, X.; Liu, X.-M.; Bataille, C. P.; Su, N. Response of the Changjiang (Yangtze River) water chemistry to the impoundment of Three Gorges Dam during 2010−2011. *Chem. Geol.* **2018**, *487*, 1−11.
(65) Li, M.; Xu, K.; Watanabe, M.; Chen, Z. Long-term variations in dissolved silicate, nitrogen, and phosphorus flux from the Yangtze River into the East China Sea and impacts on estuarine ecosystem. *Estuarine, Coastal Shelf Sci.* **2007**, *71*, 3−12.

https://dx.doi.org/10.1021/acs.est.0c01465
Environ. Sci. Technol. 2020, 54, 11940−11950